Inhibition and dynamics of a β-lactamase

Elings, W.

Chapter 3

β-lactamase of *Mycobacterium tuberculosis* shows dynamics in the active site that increase upon inhibitor binding

Abstract

Mycobacterium tuberculosis β-lactamase BlaC is a broad-spectrum β-lactamase that is able to convert various β-lactam antibiotics. Enzymes with low specificity are expected to exhibit active site flexibility, which could result in protein dynamics. We studied the dynamic behaviour of BlaC in solution using NMR spectroscopy. ^{15}N relaxation experiments show that BlaC in the resting state is mostly rigid on the pico- to nanosecond time scale. Saturation transfer experiments indicate that also on the high millisecond time scale BlaC is not dynamic. Using relaxation dispersion experiments at two magnetic fields, clear evidence was obtained for dynamics in low millisecond range, with an exchange rate of about 860 s^{-1}. The dynamic amide groups are localized in the active site. Upon formation of an adduct with the inhibitor clavulanic acid, extensive line broadening and duplication of NMR signals occurs, indicative of at least one additional, slower exchange process (k_{ex} < 100 s^{-1}), while also loss of pico- to nanosecond time scale rigidity is observed for some amides in the α-domain. Possible sources of the observed dynamics, such as motions in the omega loop and rearrangements of active site residues and hydrogen bonds, are discussed.

Introduction

A central question in chemical biology is how enzymes can have broad specificity. Enzymatic catalysis depends on efficient binding of the substrate to the enzyme and on the precise positioning of active site residues to lower the energy of a transition state. Substrates that are structurally diverse, however, have different transition states and may thus require different active site conformations to stabilize their transition states.[76–78,81,83,144–147] This implies a trade-off between active site rigidity for minimal entropic loss upon substrate binding and flexibility for adaptation to various substrates. However, substrate binding typically occurs on the millisecond time scale, whereas bond cleavage and formation events occur many orders of magnitude faster.[148] Protein motions can

likewise occur on a broad range of time scales. It can be hypothesized that enzymes that combine high catalytic efficiency with broad specificity do so by combining high rigidity on short time scales with flexibility on longer time scales. Dynamics studies on Ambler class A β-lactamases TEM-1 and PSE-4 suggest that this is true for this protein class, as is reviewed in Chapter 1.

Studies regarding the dynamics of β-lactamase / ligand complexes, however, have been scarce. Recently, the cleavage of ceftriaxone by the extended spectrum class A β-lactamase BlaC was followed from 30 ms to 2 s in near atomic detail through the acquisition of four crystallographic snapshots by a novel method called Mix and Inject Serial Crystallography.[149] The snapshots give precise structural information about the processes involved in catalysis, but the dynamic information they provide is limited to the time scale of acquisition. NMR dynamics experiments could potentially provide much more insight into the dynamic behaviour of such complexes, but as such experiments tend to take up to several days, monitoring the normal catalysis of substrates this way is not feasible. However, β-lactamases can be inhibited. Inhibition of β-lactamases has been an important clinical approach for decades and is, moreover, gaining in relevance with the increased prevalence of antibiotic resistance. In Chapter 2, the time scale of interaction between BlaC (Figure 1.3) and the inhibitor clavulanic acid was characterised in different buffers.[28] The high stability that was identified for the complex in MES buffer opens up a window for NMR dynamics measurements.

Here, we present the first NMR measurements of dynamics in BlaC and the first characterization of β-lactamase / inhibitor complex dynamics in general. We show that the dynamic behaviour of free BlaC in solution is very similar to that of other class A β-lactamases and that the rate of the active site exchange process is *ca.* 860 s^{-1} at 298 K. We also show that the high rigidity, which is a hallmark of β-lactamases, is locally lost upon inhibitor binding. Furthermore, upon binding, the effects of chemical exchange in the active site become more extensive, clearly showing that inhibitor binding changes the energy landscape of the enzyme significantly.

Results

Resting state BlaC

The backbone amide assignment of resting state BlaC without tag was derived from the previously published assignment of the tagged protein[28] via comparison with an HNCa spectrum. In this way, 98% of the BlaC backbone H−N moieties were assigned to a resonance peak in the corresponding ^{1}H, ^{15}N transverse relaxation optimized heteronuclear single quantum coherence (TROSY-HSQC)[150] spectrum. The spectra are included in Figure S3.1, assignments can be accessed under Biological Magnetic

Resonance Bank (BMRB) ID 27888. As with the tagged protein, the four residues at hydrogen-bonding distance from the active site phosphate were the only nonproline, nonterminal residues for which backbone resonances could not be identified in the spectra. The four missing resonances, as well as the lower peak intensities of the surrounding amides (Figure 3.1), suggest that an intermediate-to-fast exchange process may be present in the active site.

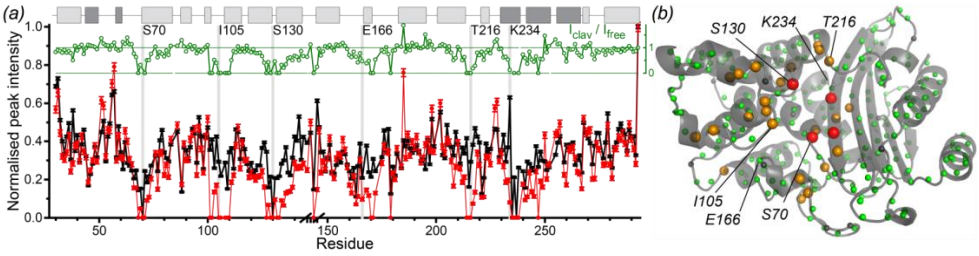

Figure 3.1. ***(a)*** **Relative peak intensities of assigned backbone amides in a $^{1}H,^{15}N$ TROSY spectrum, for resting state BlaC (black), BlaC bound to clavulanic acid (red) and the ratio between the two (green inset).** The resonance of the C-terminal amide was used for normalization. The break on the horizontal axis represents the insertion of a G-G-G-T-loop, relative to Ambler numbering. Several active site residues are indicated with grey bars. Secondary structure is indicated above the graph, light and dark grey boxes represent α-helices and β-strands, respectively. Error bars represent the spectral noise. *(b)* Visualisation of amide locations on BlaC crystal structure with PDB entry code 5NJ2. Non-proline backbone amides for which no resonance was found are indicated with red spheres. Amides for which the resonance was lost upon clavulanic acid binding are indicated with orange spheres. Amides for which a resonance could be assigned for resting state as well as bound BlaC are indicated with green spheres. Proline nitrogen atoms are indicated with grey spheres. Sphere sizes were varied between groups for emphasis.

To characterise the dynamics processes, the ^{15}N longitudinal relaxation time (T_1), ^{15}N transverse relaxation time (T_2) and the ^{15}N-{^{1}H} Nuclear Overhauser Effect (*NOE*) of the BlaC backbone amides were measured at two magnetic fields, 14 T and 20 T (Figure 3.2 and Figure 3.3, BMRB ID 27888). The obtained *NOE* ratios are high, close to and in some cases higher than the theoretical maximum, assuming an HN bond length of 1.02 Å and a chemical shift anisotropy of -160 ppm. This may be due to the 4 s relaxation time in those experiments, which was chosen based on the work of Renner *et al.*[151] and trial experiments with the model protein azurin, but may be insufficient for BlaC, as it is significantly larger.[152–154] Later experiments with ^{1}H saturation times of 6 and 10 seconds indicate that the *NOE* ratios may have been overestimated by as much as 0.025 on average. Nevertheless, the obtained *NOE* ratios show lower values for loop and surface regions of the protein and were used in further analysis. The influence of overestimated *NOE* on the resulting order parameters S^2 should be marginal, but the internal correlation times τ_e will be affected heavily and are not reported here.[155] Lipari-Szabo model-free analysis of the two-field T_1, T_2 and *NOE* data was performed using an anisotropic diffusion

tensor, yielding an average rotational correlation time of 13.9 ± 0.7 ns. This is in agreement with an estimate using HydroNMR[156] and crystal structure 5NJ2[28] (14.5 ns). Fitting of the spectral densities resulted in an average order parameter over 0.9 and yielded very few dynamic regions, confirming that BlaC is rigid on the short time scales (Figure 3.4). Most amides were best fitted with anisotropic models 1-4. Only for Val80, model 5, including an extra local order parameter S_f^2 for very fast motion, was used to fit the data (BMRB ID 27888). The resulting order parameters are S_f^2 = 0.79 ± 0.03 and S^2 = 0.57 ± 0.02, the latter of which is the lowest order parameter in the protein. The other regions that exhibit some flexibility correspond with elements that are expected to be flexible based on the crystal structure, such as the loop between β-strands 1 and 2 and that between α-helices 7 and 8.

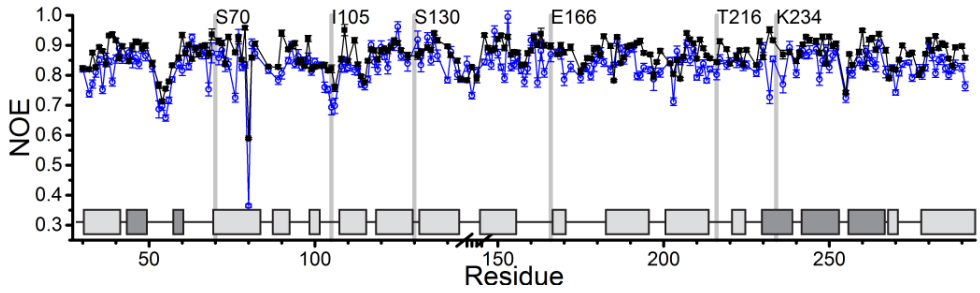

Figure 3.2. ^{15}N-{^{1}H} *NOE* of BlaC backbone amides, as measured at 20 T (black) and 14 T (blue). The break on the horizontal axis represents the insertion of a G-G-G-T-loop, relative to Ambler numbering. Error bars represent two times the standard deviations based on error propagation from the spectral noise. Several active site residues are indicated with grey bars. Secondary structure is indicated above the x-axis, light and dark grey boxes represent α-helices and β-strands, respectively. Values can also be accessed under BMRB ID 27888.

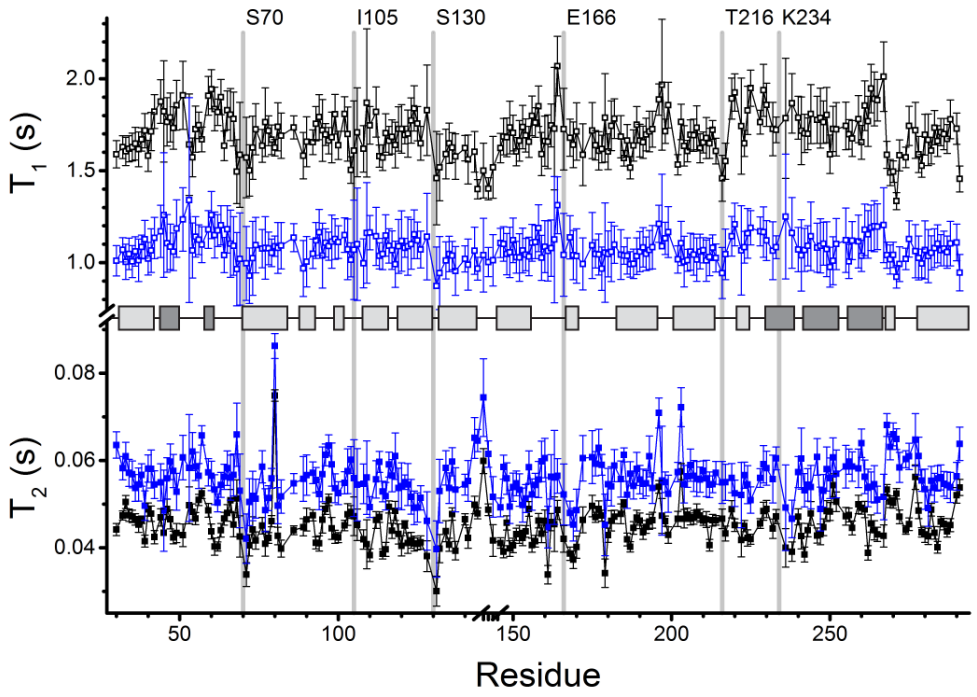

Figure 3.3. T_1 (open symbols) and T_2 (closed symbols) relaxation times of resting state BlaC backbone amides, at 20 T (black) and 14 T (blue). The break on the horizontal axis represents the insertion of a G-G-G-T-loop, relative to Ambler numbering. Several active site residues are indicated with grey bars. Secondary structure is indicated over the y-axis break, light and dark grey boxes represent α-helices and β-strands, respectively. Error bars represent the 95% confidence interval of the fit. Values can also be accessed under BMRB ID 27888.

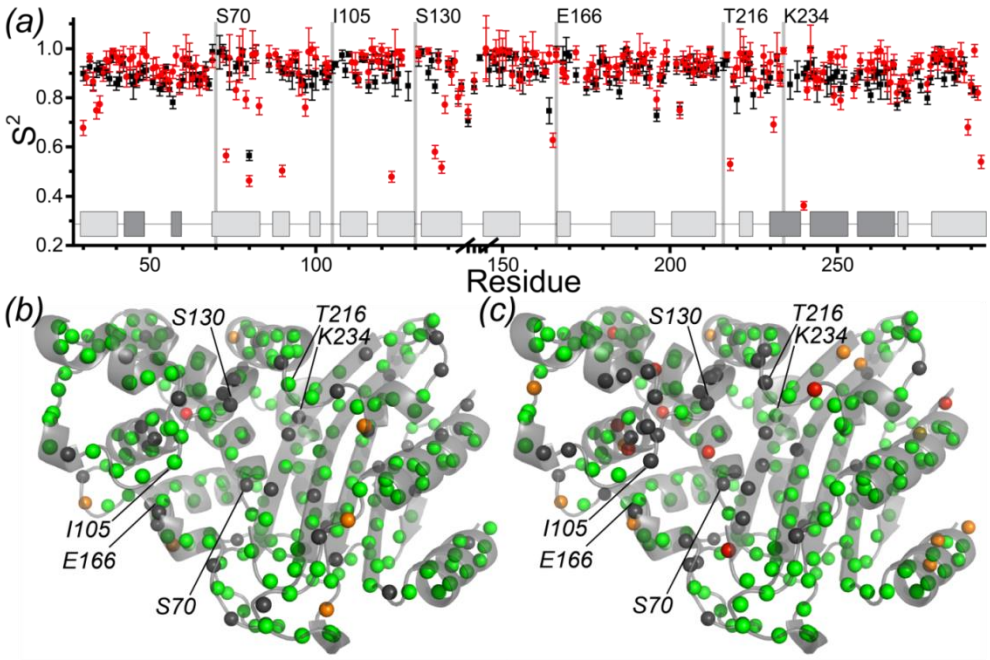

Figure 3.4. Backbone amide order parameter S^2. *(a)* S^2 values of BlaC resting state (black) and bound to clavulanic acid (red). Order parameters for resting state BlaC were obtained from per-residue fit with the best fitting anisotropic Lipari-Szabo model-free model to T_1, T_2 and NOE data from two magnetic fields. Order parameters for inhibitor-bound BlaC were obtained from similar fits to data from only one magnetic field and should therefore be interpreted as indicative. Error bars indicate the standard error of the fit. Several active site residues are indicated with grey bars. Secondary structure is indicated above the x-axis, light and dark grey boxes represent α-helices and β-strands, respectively. Values can also be accessed under BMRB IDs 27888 (free state) and 27890 (bound state). Low order parameters are indicated on the structure for BlaC in resting state *(b)* and bound to clavulanic acid *(c)*. Backbone amides with an order parameter $S^2 > 0.8$ are indicated as green spheres, those with $0.6 < S^2 < 0.8$ as orange spheres, those with $S^2 < 0.6$ as red spheres and those for which no S^2 could be determined with grey spheres.

Several residues could not be modelled without the inclusion of a chemical exchange parameter (BMRB ID 27888, residues for which Models 3 or 4 were used in the fit), so the possibility of exchange on the millisecond time scale was examined using CPMG relaxation dispersion measurements at 14 T and 20 T. Dispersion of relaxation over the pulse frequency, indicating millisecond chemical exchange, was observed to centre clearly around the active site (Figure 3.5, spheres in red and orange).

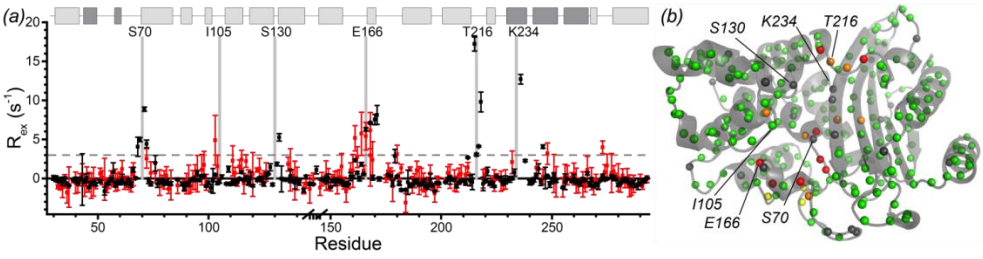

Figure 3.5. *(a)* Contribution of chemical exchange to the R_2 relaxation of backbone ^{15}N resonances in BlaC resting state (black) and bound to clavulanic acid (red), as measured by CPMG relaxation dispersion analysis. R_{ex} is defined as the $R_{2,eff}$ at ν_{CPMG} = 25 s^{-1} minus that at 1000 s^{-1}. Error bars represent the 95% confidence interval based on three duplicate delays per experiment. The break on the horizontal axis represents the insertion of a G-G-G-T-loop, relative to Ambler numbering. Several active site residues are indicated with grey bars. Secondary structure is indicated above the graph; light and dark grey boxes represent α-helices and β-strands, respectively. Values can also be accessed under BMRB IDs 27888 (free state) and 27890 (bound state). *(b)* Visualization of resting state BlaC R_{ex} on structure 5NJ2.[28] Backbone amides whose relaxation dispersion profiles were used in the group fit are displayed as red spheres and others for which $R_{ex} \geq 3$ s^{-1} as orange spheres. Residues for which the relaxation dispersion profiles suggest possible exchange in the 10^3 – 10^4 s^{-1} time scale are displayed as yellow spheres, others with $R_{ex} < 3$ s^{-1} as green spheres and those for which R_{ex} could not be determined as grey spheres.

Various types of relaxation dispersion curves were obtained. Examples are provided in Figure 3.6. Eight active site residues that showed similar dispersion profiles at both magnetic field strengths were used in a group fit (Figure 3.6 panels *(a)* – *(h)*, shown in Figure 3.5 as red spheres) yielding a chemical exchange rate of $(8.6 \pm 0.6) \times 10^2$ s^{-1}. The excited state population could not be determined with any accuracy (50 ± 50 %). A second profile shape was observed for residues Arg161, Ala164 and Asp179 (Figure 3.6, panel *(i)* and Figure S3.2, panels *(a)* – *(c)*). The contribution of this process to the affected relaxation rates was insufficient to determine the exchange rate adequately, but fits to the individual profiles suggest an exchange rate of *ca.* 10^3 – 10^4 s^{-1} (not shown). The similarity of the dispersion profiles and their co-localisation in the base of the Ω-loop (Figure 3.5, spheres in yellow) suggest that a second process may exist.

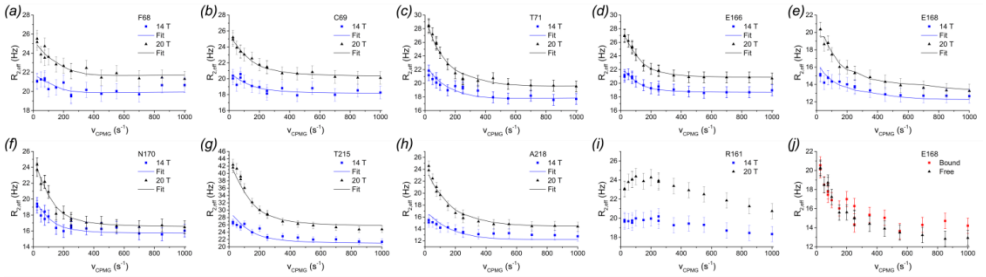

Figure 3.6. *(a)* – *(h)* Relaxation dispersion profiles that were used in a global, two-field fit yielding k_{ex} = (8.6 ± 0.6) × 10^2 s^{-1}. *(i)* Relaxation dispersion profile of Arg161, suggesting exchange on the 10^3 – 10^4 s^{-1} time scale. *(j)* Overlay of relaxation dispersion profiles of Glu168 in free form (black, same as panel *(e)*) and in clavulanic acid-bound form (red), as measured at 20 T. Error bars in all panels show the standard deviation of ±0.8 s^{-1} that was used to avoid over-fitting of ^{15}N offset-induced artefacts.

To investigate the possibility of even slower dynamic processes, chemical exchange saturation transfer (CEST) in resting state BlaC was also measured. Experiments with saturation fields of 25 Hz and 8 Hz and at temperatures of 298 K and 288 K all failed to reveal chemical exchange for any of the residues, suggesting that no significant dynamics in the CEST time scale of 20 - 200 s^{-1} are present. An example profile is provided in Figure S3.3.

Inhibitor-bound BlaC

The effect of BlaC inhibition on its dynamic behaviour was studied by performing NMR experiments on 0.38 mM BlaC with 100 mM clavulanic acid. Considering the ~1.2 h turnover time under these conditions,[28] this large excess of clavulanic acid allowed recording multidimensional NMR experiments on the BlaC/inhibitor complex. The ^{1}H-^{15}N TROSY-HSQC spectrum of backbone amides of BlaC bound to clavulanic acid was assigned by comparison to the spectra of resting state BlaC with additional help of an HNCa spectrum of a ^{15}N, ^{13}C labelled BlaC-clavulanate sample to confirm the assignments. The assignments are available at BMRB ID 27890.

Several peaks that are visible in the spectrum of resting state BlaC broaden beyond detection upon binding with clavulanic acid (Figure 3.1). These peaks all correspond to amides surrounding the binding site, indicating that the reaction with clavulanate induces enhanced chemical exchange broadening in the active site. Furthermore, at least 21 resonances were found to split into two or more distinct peaks. These peaks belong to amides around the active site and in the α-domain (Figure 3.7).

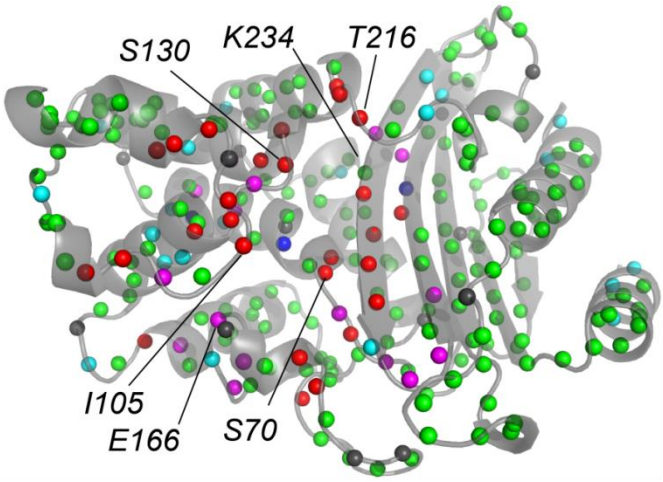

Figure 3.7. Dynamics of BlaC upon reaction with the inhibitor clavulanic acid. Backbone amides for which the resonance has broadened beyond detection are displayed in red, those for which multiple resonances could be assigned in magenta, those for which an order parameter $S^2 < 0.8$ was found in cyan, those for which the cyan and magenta conditions are both true in blue and those for which no severe dynamics were detected in green. Prolines amides are displayed in black.

The T_1, T_2 and *NOE* of clavulanate-bound BlaC were measured at 20 T (Figure S3.4 and Figure S3.5). A rotational correlation time τ_c of 16 ± 1 ns was obtained. This is significantly higher than the value for resting state BlaC, which may be caused by a change in viscosity upon the addition of 100 mM clavulanic acid to the buffer. This affects the absolute relaxation times of rigid amides, shifting the averages from 1.7 to 1.8 s (T_1) and from 45 to 40 ms (T_2). Interestingly, transverse relaxation rates were found to be significantly decreased for several residues in and near loops and terminal regions, as well as for six residues involved in the hydrophobic packing interface between helices 2 and 7 in the α subunit. Moreover, for these residues, the *NOE* is also lower than in the resting state BlaC (Figure S3.4). Lipari-Szabo model-free analysis indicates a severe decrease in rigidity in the afore-mentioned regions (Figure 3.4 and Figure 3.7). As these analyses were based on data at only one field strength and the BlaC diffusion tensor was found to be anisotropic, we would caution against over-interpreting the more detailed modelling results. Nevertheless, the data clearly indicate local loss of internal rigidity, particularly in loop regions and on the interface between helices 2 and 7.

CPMG relaxation dispersion measurements at 20 T were also performed on clavulanate-bound BlaC. However, most of the resonances that show exchange broadening in the resting state protein were broadened beyond detection in the clavulanate-bound spectra. Moreover, due to the splitting of peaks and the gradual appearance of molten globule-like background signal over time, accurate lineshape fitting of the resonances proved impossible in many cases. Residues Glu168 and Asp273 were found to have dispersion profiles with shapes similar to the active site exchange of the resting state protein (e.g.

Figure 3.6, panel *(j)*). Likewise, Arg161 showed dispersion similar to the putative faster exchange profiles (Figure S3.2, panel *(d)*). Slight elevations in the R_{ex} are observed around the loop containing Ile105, near the base of the Ω-loop and for residue Asp273, but overall the profile of exchange relaxation over all residues, keeping in mind the larger error and the missing data, looks rather similar to that of resting state BlaC (Figure 3.5). Thus, it seems that the resting state BlaC dynamics are still present upon formation of the clavulanic acid adduct and at the same time additional states are being populated, causing line broadening and peak splitting.

Discussion

We show that resting state BlaC is mostly rigid on the pico- to nanosecond time scale, similar to the behaviour of the other class A β-lactamases for which NMR dynamics studies have been performed, TEM-1[101–103] and PSE-4.[104] Only Val80 was found to exhibit significant fast motion, as modelled from the low *NOE* ratios and elevated T_2 relaxation times for its backbone amide. This is surprising, as this amide is located in the long α-helix 2 and the Val80 side chain does not face the outside of the protein but rather the interface between helices 2 and 7. The BlaC active site exhibits flexibility on the millisecond time scale, as observed by both CPMG relaxation dispersion studies and the broadening beyond detection of several important active site residues (Ser70, Ser130, Thr235 and Thr237). This behaviour is also similar to that of other class A β-lactamases,[101–110] and the localization of this chemical exchange in the active site suggests that the dynamics may play a role in catalysis. This can only be the case if the dynamics are as fast as or faster than the maximum catalytic turnover rate of the enzyme. This is the first time that the exchange rate of any serine β-lactamase active site was determined based on two-field CPMG relaxation dispersion experiments. The observed exchange rate of $(8.6 \pm 0.6) \times 10^2$ s^{-1} -obtained under the assumption of a two-state exchange model- is faster than the fastest k_{cat} that was reported for BlaC, 111 ± 4 s^{-1} for nitrocefin hydrolysis,[18] which implies that enzyme dynamics may be relevant for catalysis. On the basis of the Bloch-McConnell equations for chemical exchange, it can be shown that at an exchange rate of 860 s^{-1}, the population of the minor state must be sizeable (15 – 50 %) for the resonances of Ser70, Ser130, Thr235 and Thr237 to broaden beyond detection. The chemical shift difference between the major and minor state must be larger than 0.1 ppm for ^{1}H and/or 1 ppm for ^{15}N at 20 T. The link between these four residues is that in every BlaC crystal structure published to date, their respective sidechains each contribute to the hydrogen bonding with either the carboxyl group of a ligand or a phosphate or acetate ion from the solvent. However, upon titration with phosphate, the resonances do not appear (Chapter 2, [28]), meaning that the binding and dissociation of phosphate cannot explain the chemical exchange broadening of these peaks. The structural change causing this effect thus remains unclear.

We also report the first dynamics study of a class A β-lactamase dynamics upon ligand binding. On the pico-nanosecond time scale the reaction with clavulanic acid leads to fast motions for various residues, notably including several that are involved in the hydrophobic packing interface between helices 2 and 7, similar to what was observed for Val80 for resting state BlaC. This result resembles the observation by Stivers *et al.* that several residues of 4-oxalocrotonate tautomerase show a decrease in the order parameter upon inhibitor binding.[157] The authors suggest that the increased flexibility of these residues serves as an entropic contribution to the overall free energy change upon binding, which may well be the same for BlaC. Structurally, an increase in fast dynamics of backbone amides generally indicates increased flexibility of the peptide bond. Many of the amides for which we observe this phenomenon are on the interface of helices 2 and 7. An increase of backbone flexibility implies reduced stability of the hydrophobic core in that region of the α-domain.

Inhibition of BlaC with clavulanic acid was accompanied by a broadening of some resonances and a doubling of others. All affected amides surround the active site. The doubling of amide resonances can indicate either slow chemical exchange occurring in a single species or the formation of various adducts, which has previously been observed with mass spectrometry (e.g. [18,28,38,158]). However, the relative intensities of assigned peak pairs are 42/58 ± 3 %, while in our hands only one major mass was observed, of +70 Da (Chapter 2, [28]). The minimum chemical shift differences between peak pairs of 0.3 and 0.027 ppm in the ^{15}N and ^{1}H dimensions, respectively, indicate that if there is exchange between the states, the exchange rate must be lower than 100 s^{-1}.

Such a low exchange rate cannot explain the broadening beyond detection of the neighbouring peaks in a two-state model. However, three peaks were assigned to Ala248 and multiple other peaks are observed in the 2D TROSY that were too weak in the 3D HNCa to be assigned confidently to a spin system. These observations indicate that the two-state model does not apply. It is possible that slow exchange between more than two states could explain the broadening beyond detection of many resonances around the active site. Alternatively, multiple motions could take place on different time scales in the same region of the protein. The relaxation dispersion profile of Glu168, which is similar in free and bound form (Figure 3.6, panel *(j)*), suggests the latter. This implies that the chemical exchange processes that we observe for BlaC in the bound state are introduced in addition to the existing active site exchange process in resting state. It is clear that the binding of clavulanic acid leads to a major increase in millisecond dynamics in and around the active site of BlaC. The motion affects the chemical environment of all the catalytic residues as well as residues in all the nearby regions.

The question arises how a clavulanic acid adduct of a mere 70 Da (5 heavy atoms) can have such a major impact on such a broad region of the protein. For related β-lactamases,

it has been suggested (e.g. [102,104,106]) that the process underlying the chemical exchange effects is movement of the tip of the omega-loop into and out of the active site. Such movement could facilitate the flow of solvent and substrate, and aid in positioning of the substrate in the active orientation. This is a plausible model and it may well be true for BlaC. If so, it seems likely that the introduction of an adduct in the active site could slow down the transition from open to closed state due to steric repulsion. Amides in all regions that are in contact with the tip of the Ω-loop, such as helix 7 and the loops containing Ser130 and Ile105, would be affected by such motion. This model thus fits well with our data. A loss of hydrogen bonds between the Ω-loop and the α-domain could even explain the increased fast motions that we observe for some of the residues there. However, the implied shift from the closed towards the open state upon inhibitor binding runs counter to recent observations by Sagar *et al.*.[159] They reported an unexpectedly large solvation radius for free BlaC in solution, while BlaC bound to clavulanic acid was found to have a solvation radius closer to that which is expected based on the crystal structure. The authors proposed that free BlaC in solution adopts an 'open' conformation, whereas inhibitor binding locks BlaC in the 'closed' conformation that is observed in all crystal structures so far. If resting state BlaC were indeed to adapt an open conformation in solution, it would likely exhibit a larger rotational correlation time than in the canonical closed conformation. We observed the opposite, an increase of the correlation time upon formation of the adduct. However, the experimental rotational correlation time may have been affected by a change in buffer viscosity upon addition of 100 mM clavulanic acid to form the adduct. Thus, the data presented here provide no evidence for an open state of free BlaC, but can also not falsify such a model.

To gain more insight into what the various states may structurally look like, we compared two crystal structures of BlaC in free form (PDB entry codes 5NJ2 and 5OYO[28]) with those of BlaC bound to clavulanic acid adduct (3CG5,[130] 6H2C and 6H2G[160]). Small differences between the individual structures, such as sub-Ångström rearrangements of the active site residues or the Ω-loop backbone, can be identified. Surprisingly, however, none of these differences are consistent within the two ensembles of free and clavulanate-bound BlaC. This lack of clustering is also reflected by the root mean square deviation of the alignment of the two free structures to each other (0.5 Å), which is not smaller than those for the three clavulanate-bound structures to free structure 5NJ2 (0.4, 0.2 and 0.8 Å, respectively). Recently, Olmos *et al.*[149] reported an XFEL study with snapshots at 30, 100, 500 and 2000 ms of the catalytic reaction of ceftriaxone hydrolysis by BlaC. The structures obtained during the reaction show almost no structural variation compared to that of BlaC in the resting state. The only active site residues of which the orientation varies between the structures are Lys73 and Ser130. Vandavasi *et al.* used neutron and X-ray crystallography to study the role of Lys73 in class A β-lactamase PenP and observed it to adopt two conformations upon ligand binding,[20] similar in orientation to the two

conformations observed for BlaC by Olmos *et al*. One of these conformations allows an extra water molecule to penetrate deep into the active site, between helix 2 (Lys73) and helix 7 (Met135, which is an alanine in BlaC). The occupancies of these states, 41 and 59 %, respectively, match the relative occupancies of the doubled peaks of 42 ± 3 % that we observe in our spectra. As mentioned before, if there is chemical exchange between the states in our spectra, the rate must be lower than 100 s^{-1}. Although this seems very slow for any movement as small as a sidechain reorientation, the fact that the two Ly73 states were distinguishable in crystal structures at 293 K as well as at 15 K does point towards the two states being highly stabilized relative to the transition states, implying that exchange should indeed be very slow. It therefore seems possible that the chemical exchange we observe upon clavulanic acid binding is related to the interconversion of Lys73 between different conformations and protonation states and is thus, as Olmos *et al.* argued, involved in proton transfer between Lys73 and Ser130.

In conclusion, we show that BlaC is highly rigid on the pico-nanosecond time scale, but exhibits flexibility on the millisecond time scale in and around the active site, with an exchange rate of *ca.* 860 s^{-1}. The dynamic behaviour of free BlaC is very similar the other class A β-lactamases for which dynamics studies were performed and therefore appears to be conserved amongst class A β-lactamases. The high rigidity minimises the entropic cost of binding, while flexibility allows adaptation to various substrates on the time scale of diffusion. We also show that upon binding to the inhibitor clavulanic acid, the prevalence of dynamics around the active site increases dramatically on both the millisecond and pico- / nanosecond time scales.

Materials And Methods

Materials

Pure BlaC without signal peptide and without purification tag (sequence detailed in Figure S2.3) was obtained as described previously.[28] The Ambler standard β-lactamase numbering scheme (Figure S2.3) is used throughout this thesis.[17] Clavulanic acid from manufacturer Matrix Scientific was used, concentrations were determined using the previously determined extinction coefficient at 256 nm of 20.0 (0.1) mM^{-1} cm^{-1}.[28]

Methods

Unless mentioned otherwise, all experiments were performed on samples containing 0.38 mM ^{15}N enriched BlaC in 94 mM MES/NaOH pH 6.4 and 6% D_2O, at 298 K. Measurements of BlaC bound to clavulanic acid were performed on samples obtained by mixing BlaC with clavulanic acid in the same buffer, ~1 h before the start of the acquisition to concentrations after mixing of 0.38 mM BlaC and 100 mM clavulanic acid, unless mentioned otherwise. NMR spectra were recorded on Bruker AVIII HD 850 MHz (20 T) or

Bruker AVIII 600 MHz (14 T) spectrometers equipped with a TCI cryoprobe or a TXI probe, respectively. HNCa spectra were measured on samples containing 0.7 mM $^{15}N^{13}C$ enriched BlaC (free) or 0.4 mM $^{15}N^{13}C$ enriched BlaC and 186 mM clavulanic acid, in the same buffer. These spectra were recorded using standard Bruker pulse program 'trhncaetgp3d', processed with Topspin 3.2 (Bruker Biospin, Leiderdorp) and analysed using CCPNmr Analysis.[143] *NOE* measurements were performed using standard Bruker pulse program 'hsqcnoef3gpsi' or to the sequence as detailed by Cavanagh *et al.*[89], with a ^{1}H saturation delay of 3 or 4 s. T_1 measurements were performed using standard Bruker pulse program 'hsqct1etf3gpsitc3d', with a recycle delay between experiments of 6 s and variable delays of 0.12, 0.17, 0.24 (2x), 0.33, 0.46, 0.65, 0.91, 1.28 (2x), 1.78 and 2.50 s. T_2 measurements were performed using standard Bruker pulse program 'hsqct2etf3gpsitc3d', with a recycle delay between experiments of 4 s and variable T_2-delays of *ca.* 0, 17, 34 (2x), 51, 68, 85, 102, 119 (2x), 136 and 153 ms. T_1 and T_2 data were processed with Topspin 3.2 and resulting peak heights were fitted to exponential decay curves using Dynamics Center 2.5 (Bruker BioSpin, Rheinstetten). *NOE* data were processed and analysed with the same software.

Lipari-Szabo analysis was performed with Dynamics Center 2.5. The rotational correlation time τ_c was calculated with Equation 3.1[161] and averaged over all residues for which the *NOE* > 0.75 and T_1 and T_2 were each within one standard deviation of their respective means. The experimental correlation time was compared with an estimate based on the crystal structure using HydroNMR[156] and subunit A of crystal structure 5NJ2, after deletion of the histidine tag and linker from the pdb file.

Equation 3.1.

$$\tau_c = \frac{1}{2 \times \omega_N} \times \sqrt{\frac{6 \times T_1}{T_2} - 7}$$

Least-squares fitting of the reduced spectral density function $J(\omega)$ to the relaxation parameters was performed with 1000 iterations with random starting parameters, using an NH bond length of 1.02 Å and an average chemical shift anisotropy of -160 ppm. To avoid overfitting of relaxation parameters with small errors, Lipari-Szabo analyses were performed with user-defined errors of 10 % (T_1) and 5 % (T_2 and *NOE*) of the respective values. Relaxation data from each residue were fitted with the five standard anisotropic model-free models.[161,162] In Model 1, the order parameter S^2 is fitted for each residue, while the correlation times τ_j are calculated from components and orientation of the diffusion tensor, which is a global parameter. In Model 2, a local correlation time τ_e for fast motion is additionally fitted individually for each residue. Model 3 is the same as Model 1, except that an R_{ex} term is added to the R_2 in the calculation of the reduced spectral densities. Likewise, Model 4 is the same as Model 2 with the addition of an R_{ex} term. In Model 5, an extra modelling parameter S_f^2 is included for very fast local motion. The best

model was selected based on the lowest *AIC* value, which is the sum of the χ^2 of the fit and the number of fitted parameters $\times$ 2. The selected model for each residue is reported under BMRB IDs 27888 (free state) and 27890 (bound state).

CPMG relaxation dispersion measurements were performed on 0.38 – 1.0 mM ^{15}N BlaC using the TROSY CPMG pulse program as detailed by Vallurupalli *et al.*,[163] with 0, 1 (2x), 2, 3 (2x), 4, 6, 8, 10 (2x), 14, 18, 22, 28, 34 and 40 ^{15}N 180° pulses in 40 ms relaxation time, respectively. Data were processed with NMRPipe[164] and resulting resonances were fitted to a glore lineshape using FuDa.[165] Effective transverse relaxation rates $R_{2,eff}$ were calculated from the fitted peak heights using $R_{2,eff}(\nu_{CPMG}) = -ln(I(\nu_{CPMG}) / I_0) / T_{ex}$. In the relaxation dispersion data of BlaC bound to clavulanic acid, a few profiles showed ^{15}N-offset dependent variations that were much bigger than the experimental noise (examples in Figure S3.2, panels *(e)* and *(f)*). This variation is likely due to technical imperfections, so these data points were excluded from Figure 3.5 and BMRB ID 27890. An exclusion cut-off of 10 s^{-1} total increase in $R_{2,eff}$ between subsequent pulse frequencies was used. Figure S3.6 shows the complete dataset, including the points that were excluded from Figure 3.5, BMRB ID 27890 and further analysis. The chemical exchange rate and excited state population of the resting state were determined with a two-field grouped fit with the software CATIA,[97] using a minimum $R_{2,eff}$ standard deviation of 0.8 s^{-1} to avoid over-fitting of small ^{15}N offset-induced artefacts.

Chemical Exchange Saturation Transfer (CEST) measurements were performed on 0.38 – 1.0 mM ^{15}N BlaC using the standard Bruker 'hsqc_cest_etf3gpsitc3d' pulse program, with 2.5 s recycle delay and 0.8 s B_1 irradiation at frequencies in the ^{15}N range 100.5:0.5:130 ppm.

Figures containing the protein structure were created using the PyMOL Molecular Graphics System, Version 2.2 Schrödinger, LLC.

Supplementary Figures

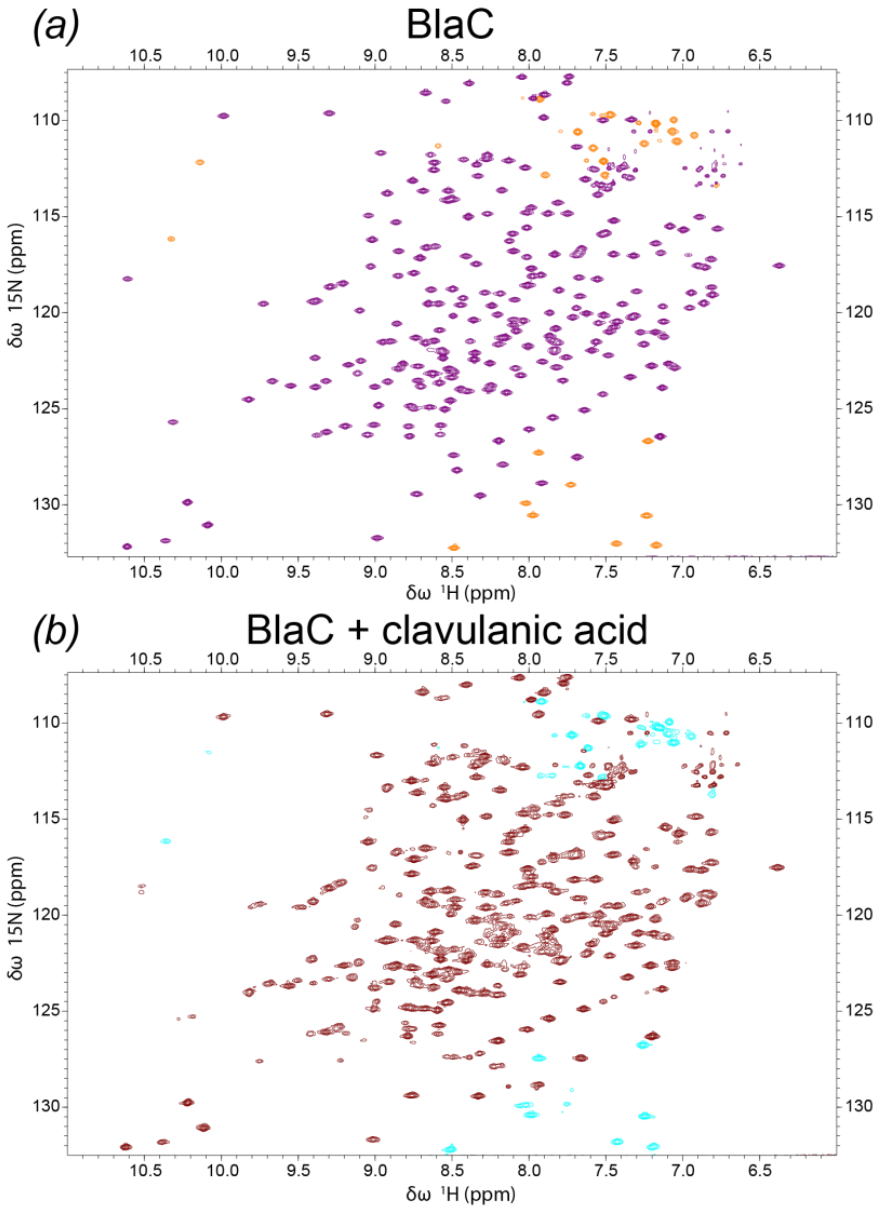

Figure S3.1. TROSY-HSQC spectra of BlaC in free and bound state. In each spectrum, contour levels in the minority colour indicate folded peaks. Assignments can be accessed under Biological Magnetic Resonance Bank IDs 27888 (free state) and 27890 (bound state).

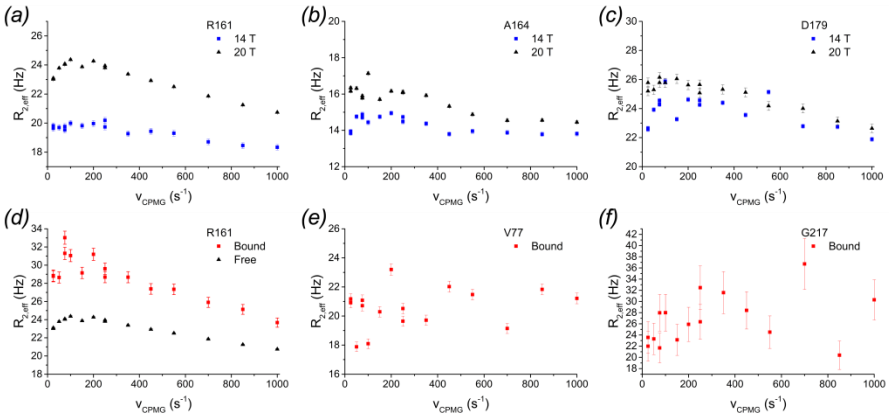

Figure S3.2. Example CPMG relaxation dispersion profiles. *(a)* – *(c)* Profiles suggesting exchange on the 10^3 – 10^4 s^{-1} time scale. *(d)* Profile suggesting that exchange on the 10^3 – 10^4 s^{-1} time scale may still be present after the binding of clavulanic acid. *(e), (f)* Examples of profiles that were excluded from Figure 3.5 and BMRB ID 27890 due to technical artefacts. Data in panels *(d)* – *(f)* were acquired at 20 T. Error bars in all panels represent the standard deviation based on three replicate pulse frequencies.

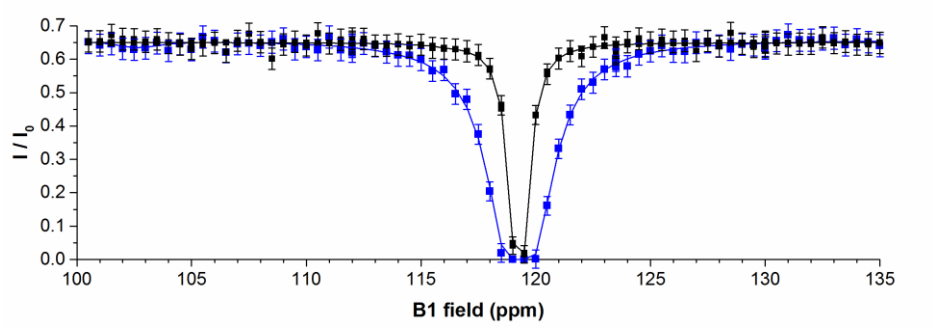

Figure S3.3. Example CEST curves for Glu166, as measured at 298 K with B_1 field strengths of 8 Hz (black) and 25 Hz (blue), respectively. Error bars represent the 95% confidence interval as derived from the spectral noise; lines are drawn to guide the eye. No secondary dips were observed.

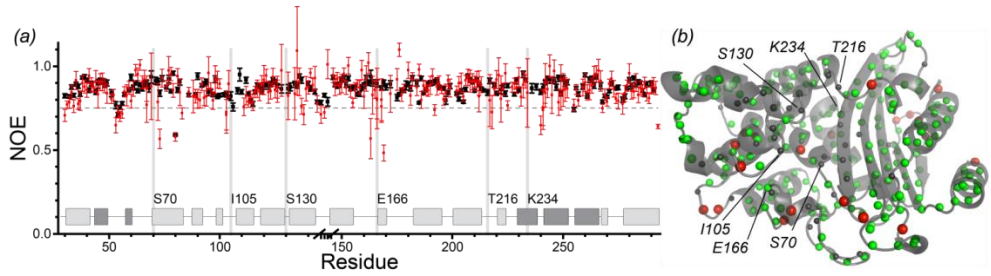

Figure S3.4. ***(a)*** **^{15}N-{^{1}H}** ***NOE*** **of backbone amides, as measured at 20 T for BlaC in resting state (black) and bound to clavulanic acid adduct (red).** Several active site residues are indicated with grey bars. The break on the horizontal axis represents the insertion of a G-G-G-T-loop, relative to Ambler numbering. Secondary structure is indicated above the x axis, light and dark grey boxes represent α-helices and β-strands, respectively. Error bars represent the 95% confidence interval based on error propagation from the spectral noise. Values can also be accessed under BMRB IDs 27888 (free state) and 27890 (bound state). *(b)* Colour map of *NOE* upon binding of clavulanic acid. Backbone amides for which *NOE* < 0.75 are represented as red spheres, those with *NOE* ≥ 0.75 as green spheres and those for which *NOE* could not be determined as grey spheres. Sphere sizes were varied between groups for emphasis.

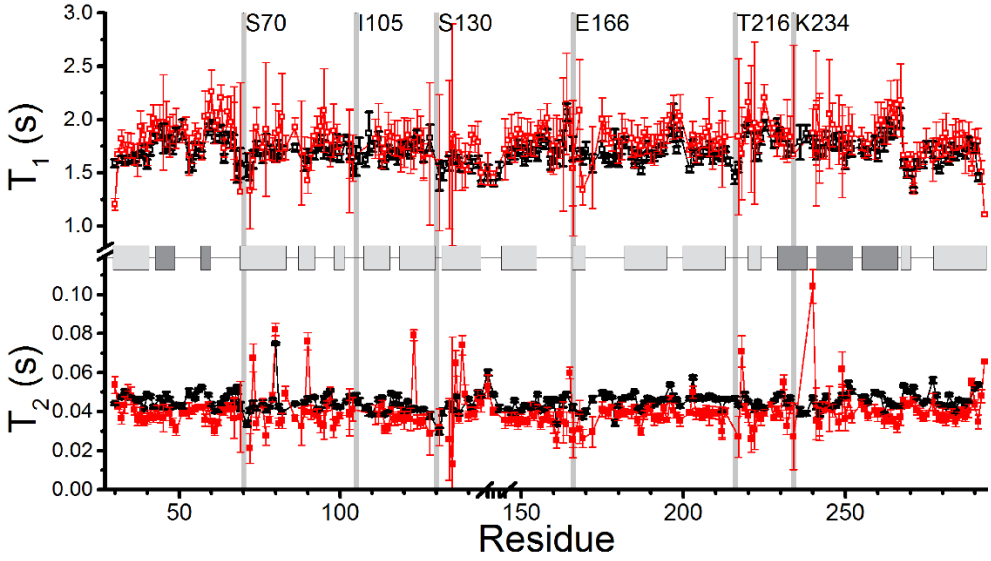

Figure S3.5. ***T_1*** **(open symbols) and** ***T_2*** **(closed symbols) relaxation times of backbone amides of BlaC in resting state form (black) and bound to clavulanic acid adduct (red), measured at 20 T.** Error bars show the standard error of the fit. Values can also be accessed under BMRB IDs 27888 (free state) and 27890 (bound state). Several active site residues are indicated with grey bars. The break on the horizontal axis represents the insertion of a G-G-G-T-loop, relative to Ambler numbering. Secondary structure is indicated over the y axis break, light and dark grey boxes represent α-helices and β-strands, respectively.

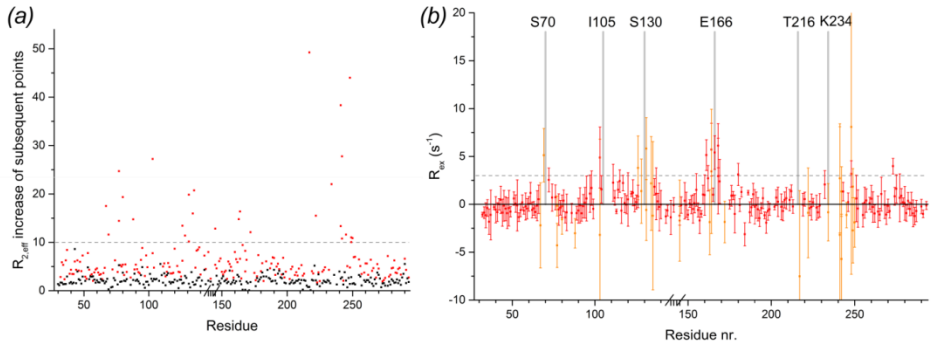

Figure S3.6. Exclusion of relaxation dispersion profiles with extremely large systematic deviations. *(a)* Plot of exclusion parameter on the protein sequence. No profiles from the resting state protein dataset (black) were excluded, 28 profiles from the clavulanic acid-bound protein dataset (red) were excluded. *(b)* Plot of resulting clavulanic acid-bound R_{ex} on the protein sequence, with data that were included in Figure 3.5 and BMRB ID 27890 in red and data that were excluded in orange. Several active site residues are indicated with grey bars for reference. Error bars represent the 95% confidence interval based on three duplicate delays per experiment.